

ARTICLE

Open Access

Oil-mediated high-throughput generation and sorting of water-in-water droplets

Lang Nan¹, Yang Cao¹, Shuai Yuan² and Ho Cheung Shum¹

Abstract

Aqueous two-phase system (ATPS) droplets have demonstrated superior compatibility over conventional water-in-oil droplets for various biological assays. However, the ultralow interfacial tension hampers efficient and stable droplet generation, limiting further development and more extensive use of such approaches. Here, we present a simple strategy to employ oil as a transient medium for ATPS droplet generation. Two methods based on passive flow focusing and active pico-injection are demonstrated to generate water-water-oil double emulsions, achieving a high generation frequency of ~ 2.4 kHz. Through evaporation of the oil to break the double emulsions, the aqueous core can be released to form uniform-sized water-in-water droplets. Moreover, this technique can be used to fabricate aqueous microgels, and the introduction of the oil medium enables integration of droplet sorting to produce single-cell-laden hydrogels with a harvest rate of over 90%. We believe that the demonstrated high-throughput generation and sorting of ATPS droplets represent an important tool to advance droplet-based tissue engineering and single-cell analyses.

Introduction

Droplet microfluidics has demonstrated vast promise in processing and analyzing biological samples due to its capacity to confine individual targets in microscale volumes and perform high-throughput manipulations^{1–4}. However, the conventional use of water-oil droplet systems is constrained by the toxic nature of organic reagents, which reduces their biocompatibility and prevents access to droplet contents⁵. With an all-aqueous environment, water-in-water droplets produced by introducing aqueous two-phase systems (ATPSs) have attracted growing interest and shown great potential in fabricating biomimetic architectures^{6,7}.

ATPS is typically an aqueous solution of two incompatible polymers or one polymer and one salt, which phase-separates to form two immiscible phases when the

concentrations exceed their corresponding critical values⁸. The potential biocompatibility has promoted ATPSs as a promising candidate for various biological assays, including cell culture⁹, protein delivery¹⁰, and DNA partitioning¹¹, but a strategy to generate water-in-water droplets is needed. To form droplets with uniform shapes and sizes, the two phase-separated immiscible phases are conventionally introduced into microfluidic channels for droplet formation¹². However, interfaces of two aqueous phases can possess ultralow interfacial tension (typically in the range of $10^{-4} \sim 10^{-1}$ mN/m), challenging the efficient and stable generation of droplets in microfluidic systems: The droplets can be formed only under ultralow flow rates (below $3 \mu\text{L/h}$) at frequencies below 10 Hz, and the droplet size distribution is also undesirably large¹³. Moreover, when polyelectrolytes or nanoparticles are added to stabilize the droplets, their fast assembly at the interface hampers pinch-off of the interface, further lowering the generation efficiency^{14,15}.

To improve the droplet generation efficiency, active actuation strategies have been employed; by providing additional energy, pinch-off of the interfaces can be

Correspondence: Ho Cheung Shum (ashum@hku.hk)

¹Department of Mechanical Engineering, The University of Hong Kong, Pokfulam Road, Hong Kong, China

²Department of Electrical and Electronic Engineering, The University of Hong Kong, Pokfulam Road, Hong Kong, China

These authors contributed equally: Lang Nan, Yang Cao

© The Author(s) 2020



Open Access This article is licensed under a Creative Commons Attribution 4.0 International License, which permits use, sharing, adaptation, distribution and reproduction in any medium or format, as long as you give appropriate credit to the original author(s) and the source, provide a link to the Creative Commons license, and indicate if changes were made. The images or other third party material in this article are included in the article's Creative Commons license, unless indicated otherwise in a credit line to the material. If material is not included in the article's Creative Commons license and your intended use is not permitted by statutory regulation or exceeds the permitted use, you will need to obtain permission directly from the copyright holder. To view a copy of this license, visit <http://creativecommons.org/licenses/by/4.0/>.

triggered. For instance, with the assistance of acoustic vibration and oil chopping to destabilize the jet, the generation frequency can be increased two-fold in comparison to passive generation in glass-capillary devices^{16,17}. Polydimethylsiloxane (PDMS) devices with typically two-dimensional planar geometries are often used, where more sophisticated droplet manipulation is enabled, for instance, droplet sorting¹⁸ and pico-injection¹⁹. However, the shear force in these geometries dampens the active actuation, which becomes less effective in generating droplets with a high throughput²⁰. As a result, even with mechanical actuation and eight parallel channels, the highest production rate is only approximately 100 Hz, which is still inefficient compared with water-in-oil droplet generation, typically with rates on the order of kHz²¹. Moreover, due to the similar electrical properties of the two aqueous phases, electrical manipulations of the generated droplets, such as dielectrophoretic (DEP)-based droplet sorting²², fail to work and preclude certain sample processing and analysis steps.

To address these problems, we propose an oil-mediated strategy to generate ATPS droplets, where water-water-oil double emulsions are first generated, with the inner aqueous cores subsequently released to form water-in-water droplets. To demonstrate the efficiency of this approach, double emulsions are passively generated in a flow-focusing channel at high throughput and with a uniform size distribution. The use of a transient oil medium also enables electric actuation to further increase the droplet generation rate and degree of control of the generated droplets. To extract the inner aqueous droplets, the transient oil layer is evaporated in a gentle and efficient manner. Through further incorporation of sodium alginate and integration of a droplet sorting system, single-cell-laden hydrogels can be produced, with a high harvest rate.

Results

Passive double-emulsion generation

As the first step in ATPS droplet formation, the generation of water-water-oil double emulsions determines the final droplet size and morphology. To generate monodisperse double-emulsion drops, we passively break up the aqueous flow into droplets by oil pinching, which can be achieved in a typical multi-inlet flow-focusing channel²³. Different from the water-oil-water (W-O-W) double-emulsion drops that are formed by two steps of emulsification²⁴, water-water-oil (W-W-O) double-emulsion drops are formed in a single step at the second cross junction: The two aqueous phases flow lamina-ly side-by-side after meeting in the first junction, followed by pinch-off of the water-water compound jet by the oil flow to form W-W-O double-emulsion drops (Fig. 1a and Movie S1). To demonstrate the efficiency of this

method, the two most commonly used ATPS polymers, polyethylene glycol (PEG) and dextran (DEX) that are both biocompatible, are introduced. To prevent coalescence and destabilization of the droplets during subsequent droplet extraction, two oppositely charged polyelectrolytes, poly(allylamine hydrochloride) (PAH) and poly(sodium 4-styrenesulfonate) (PSS), are dissolved into the innermost (DEX-rich) and intermediate (PEG-rich) solutions to stabilize the water-water interface through interfacial complexation. However, due to the fast reaction, premature precipitation prior to droplet breakup tends to gradually block the channel and cause a transition from the original dripping regime to an unstable jetting regime within 3 min. Thus, a spacing stream of pure PEG-rich solution is introduced at a flow rate of 100 $\mu\text{L}/\text{h}$ to separate the two reagent streams, thereby enabling stable droplet generation for over 1 h and forming monodisperse double emulsions (Fig. 1b, c).

To optimize the microfluidic operations for controllable double-emulsion generation, the droplet size and generation frequency at different flow conditions are systematically studied. In this flow regime, the two streams of PEG-rich phases with and without PSS converge into one stream before droplet generation, and varying the flow rate ratio between the two PEG-rich phases does not lead to any observable effect on the resultant droplet size (Fig. S1). Thus, in the following analysis, we use the combined flow rate to characterize the flow behaviors. First, by regulating the flow rates of the aqueous phases, the formed core-shell structure can be controlled. We change the flow rate ratio of the DEX-rich phase and PEG-rich phase from 1:7 to 7:1 while keeping the oil flow rate constant. As a result, the inner droplet diameter increases while the outer droplet diameter remains unchanged, with the diameter ratio ranging from 50 to 96% and the resultant shell thickness varying from 26 μm to $\sim 2 \mu\text{m}$ (Fig. 1d). The flow rate of oil is a key parameter that affects both the double-emulsion drop size and generation frequency. To quantify the effect of flow rate on the double-emulsion formation, we set the flow rates of DEX-rich and PEG-rich phases constant at 200 $\mu\text{L}/\text{h}$ and 600 $\mu\text{L}/\text{h}$, respectively, while tuning the flow rate of oil from 2000 to 10,000 $\mu\text{L}/\text{h}$. For oil flow rates below 2000 $\mu\text{L}/\text{h}$, the aqueous compound jet cannot be pinched off. Experimentally, the core diameter gradually drops from 73 μm to $\sim 43 \mu\text{m}$ as the oil flow rate increases, and the generation frequency increases from 270 Hz to ~ 1200 Hz (Fig. 1e). Since the two aqueous phases are formed by phase separation of PEG and DEX solutions, the adopted polymer concentrations determine the interfacial tension and viscosity of the two aqueous phases, thus affecting the interface pinch-off and droplet breakup. To understand the effect of polymer concentrations and test the feasibility of this approach in

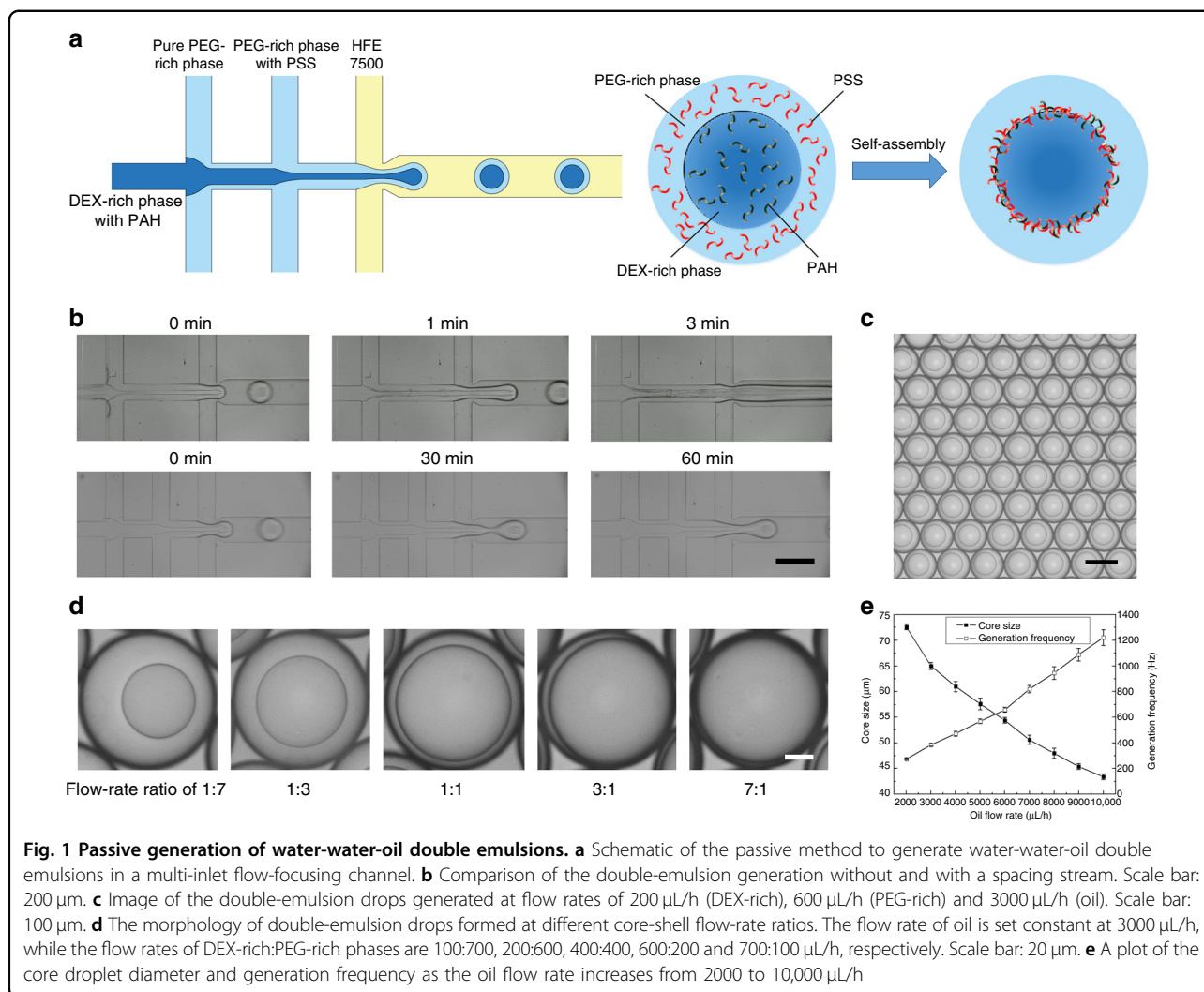


Fig. 1 Passive generation of water-water-oil double emulsions. **a** Schematic of the passive method to generate water-water-oil double emulsions in a multi-inlet flow-focusing channel. **b** Comparison of the double-emulsion generation without and with a spacing stream. Scale bar: 200 μm . **c** Image of the double-emulsion drops generated at flow rates of 200 $\mu\text{L/h}$ (DEX-rich), 600 $\mu\text{L/h}$ (PEG-rich) and 3000 $\mu\text{L/h}$ (oil). Scale bar: 100 μm . **d** The morphology of double-emulsion drops formed at different core-shell flow-rate ratios. The flow rate of oil is set constant at 3000 $\mu\text{L/h}$, while the flow rates of DEX-rich:PEG-rich phases are 100:700, 200:600, 400:400, 600:200 and 700:100 $\mu\text{L/h}$, respectively. Scale bar: 20 μm . **e** A plot of the core droplet diameter and generation frequency as the oil flow rate increases from 2000 to 10,000 $\mu\text{L/h}$

more viscous flows, we increase the PEG and DEX concentrations from 10 to 20% and measure the resultant core size and generation frequency at constant flow conditions (200 $\mu\text{L/h}$ for the DEX-rich phase, 600 $\mu\text{L/h}$ for the PEG-rich phase and 3000 $\mu\text{L/h}$ for the oil phase). The results indicate that as the polymer concentration increases, the size of the core droplets increases from 65 μm to 77 μm , and the frequency decreases from 385 to 240 Hz (Tables 1 and 2). In summary, this method enables high-throughput generation of W-W-O double emulsions with controlled structures.

Active double-emulsion generation

In addition to the demonstrated passive generation, double-emulsion drops can be actively generated by injecting the core droplet into the shell droplet one-by-one by pico-injection. Here, a typical pico-injection channel is employed for the two-step generation²⁵. In the flow-focusing junction, the PEG-rich solution is

broken up into droplets under the shear effect of the oil stream. Then, when the droplets flow by the pico-injector, a high voltage is applied to the electrodes to destabilize the water-oil interface, thus introducing the DEX-rich solution into the shell drop to form a double emulsion (Fig. 2a). This method relies on accurate control over the applied electric field, where an optimal pulse with a frequency of 10 kHz and peak-to-peak voltage of 500 V_{p-p} is applied to achieve a stable injection with identical volumes injected into each droplet²⁵.

In comparison with the passive generation that simultaneously pinches off two aqueous streams, only one stream of the PEG-rich phase is segmented in the active operations, thus allowing more frequent double-emulsion generation. To demonstrate the higher efficiency, a similar test is performed to explore the effect of the oil flow rate on the double-emulsion generation. We change the flow rate of the oil phase from 500 to 10000 $\mu\text{L/h}$, while the flow rates of the droplet phase (PEG-rich) and

injection phase (DEX-rich) are maintained at 600 and 200 $\mu\text{L}/\text{h}$, respectively. The results indicate that under the same flow conditions, smaller droplets can be generated at a higher frequency in the active mode. For instance, at the same oil flow rate of 3000 $\mu\text{L}/\text{h}$, the frequency of active generation (750 Hz) is approximately two times that of passive generation (380 Hz) (Fig. 2b). Moreover, double-emulsion formation at different polymer concentrations is studied. We set the flow rates of DEX-rich, PEG-rich and oil phases at 200, 600 and 3000 $\mu\text{L}/\text{h}$, respectively.

Table 1 The density, viscosity and interfacial tension of different concentrations of polymer solutions

Polymer solutions	Density (g/ cm^3)	Viscosity (Pa-s)	Interfacial tension (mN/m)
PEG-rich 10%	1.038	0.011	0.116
DEX-rich 10%	1.100	0.018	
PEG-rich 10%	1.036	0.014	0.157
DEX-rich 15%	1.130	0.030	
PEG-rich 10%	1.044	0.020	0.186
DEX-rich 20%	1.135	0.032	
PEG-rich 15%	1.039	0.018	0.173
DEX-rich 10%	1.127	0.033	
PEG-rich 15%	1.044	0.027	0.249
DEX-rich 15%	1.151	0.052	
PEG-rich 15%	1.048	0.034	0.394
DEX-rich 20%	1.165	0.072	
PEG-rich 20%	1.046	0.035	0.368
DEX-rich 10%	1.166	0.083	
PEG-rich 20%	1.050	0.044	0.478
DEX-rich 15%	1.179	0.123	
PEG-rich 20%	1.054	0.060	0.521
DEX-rich 20%	1.195	0.154	

Experimentally, when the concentrations of the two polymers increase from 10 to 20%, the resultant core size increases from 52 to 61 μm , and the generation frequency decreases from 750 to 480 Hz (Table 3).

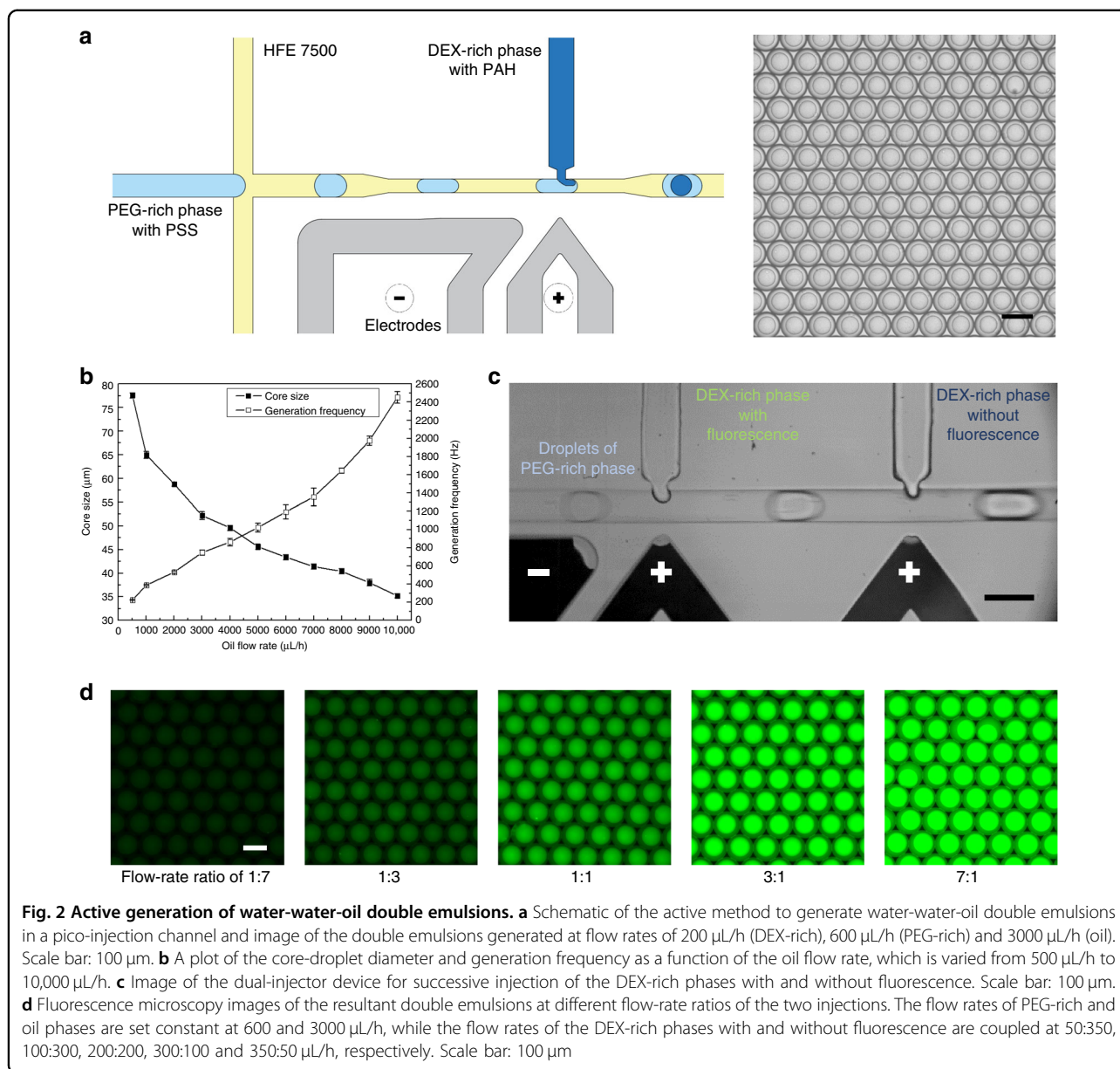
In addition to the higher efficiency, the active generation method allows injection of different ingredients into the core droplets, thereby enabling time-controlled reactions within the droplets. We achieve this aim in a dual-injector device, where the two injectors are closely located at a spacing of 500 μm to efficiently merge the injected cores before the assembly of polyelectrolytes to form a membrane at the interface. To demonstrate the efficiency of this approach, a fluorescently labeled DEX-rich solution is introduced from the first injector, while a conventional solution without fluorescent dye is introduced from the second injector (Fig. 2c). As the flow rate ratio of the two injection flows is tuned from 1:7 to 7:1, double emulsions with different fluorescence intensities can be formed, achieving good mixing to allow accurate control of the fluorescent polyelectrolyte concentration (Fig. 2d).

Core-droplet extraction

To extract the encapsulated core droplets for ATPS droplet formation, the carrier oil must be removed to break the double-emulsion drops. Typically, the droplets are broken by first adding the demulsifier to destabilize the surfactant layer and then centrifuging the samples to separate the water and oil phases based on their density difference²⁶. However, this method involves severe flow disturbance, which tends to disrupt both the water-oil interface and water-water interface, thus inducing undesirable coalescence of the ATPS droplets. Therefore, gentler extraction should be employed to break the outer droplet interface while keeping the inner droplets intact. Here, we introduce a noninvasive method that hinges on evaporation of the oil phase to break the double emulsions. This method is performed by transferring the collected emulsions into a Petri dish filled with the PEG-rich solution. When the emulsions fall onto the solution, the interfacial tension keeps the oil phase on the top, with the

Table 2 The core-droplet diameter and generation frequency at different polymer concentrations in the passive generation mode

DEX-rich	M_w 8000 (PEG-rich)						
	10%		15%		20%		
	Core size (μm)	Frequency (Hz)	Core size (μm)	Frequency (Hz)	Core size (μm)	Frequency (Hz)	
M_w 10,000	10%	65.0 \pm 0.7	385.0 \pm 10.6	66.6 \pm 0.5	362.2 \pm 7.1	73.4 \pm 0.5	267.2 \pm 3.8
	15%	68.2 \pm 0.4	331.0 \pm 4.5	72.2 \pm 0.4	282.8 \pm 4.4	74.6 \pm 0.5	253.6 \pm 3.3
	20%	70.2 \pm 0.4	315.0 \pm 4.5	74.4 \pm 0.5	264.4 \pm 3.1	76.6 \pm 0.5	239.2 \pm 2.7



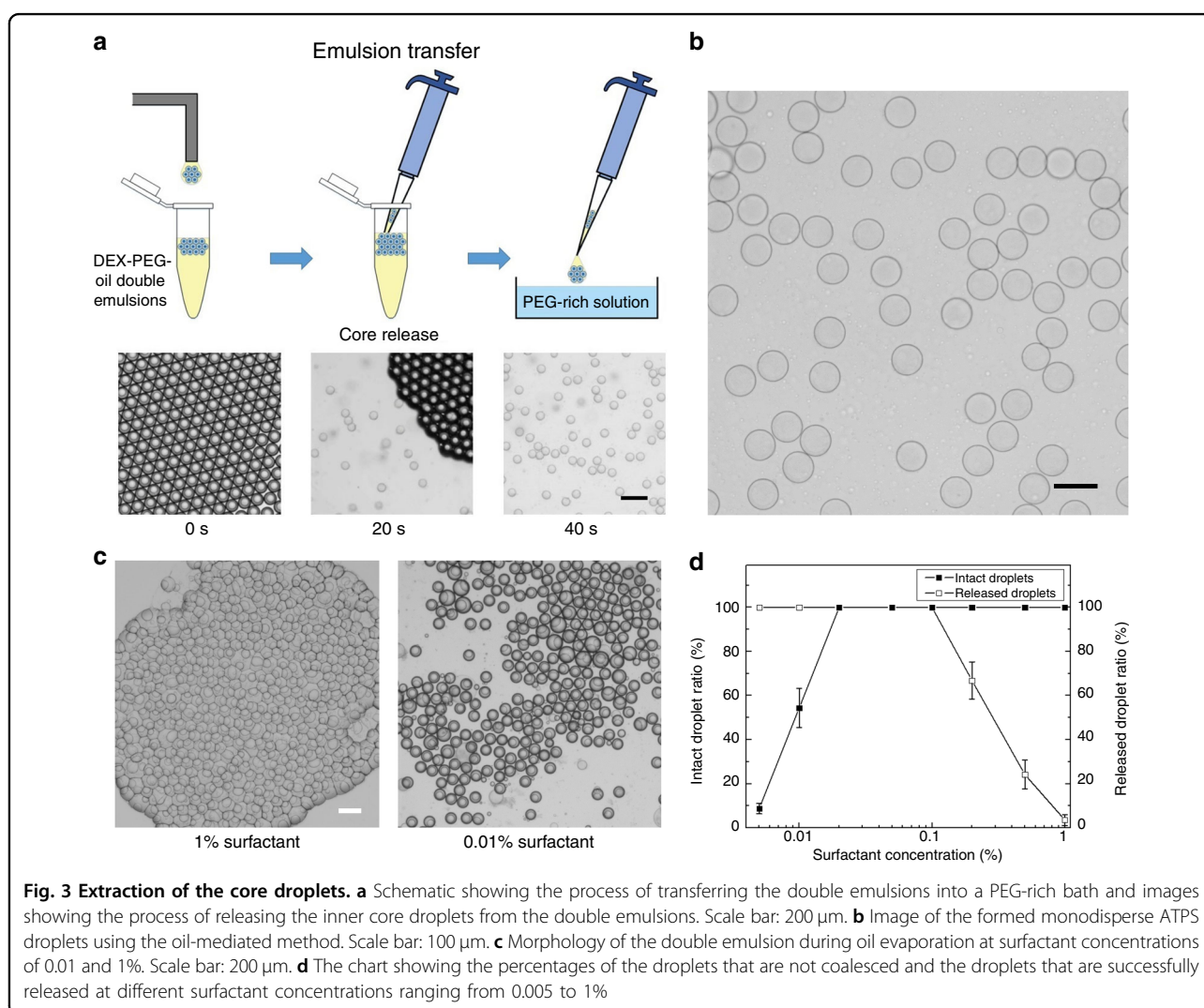
double-emulsion drops aggregating at the center. As the surrounding oil spreads and forms a thin layer, its surface area increases. Consequently, the oil layer evaporates in ~20 s, and the shell phase merges with the PEG-rich solution underneath; hence, the cores of the DEX-rich phase are released to form monodisperse DEX-in-PEG droplets (Fig. 3a, b).

In this method, the surfactant concentration is a key factor in implementing core-droplet extraction. To elucidate the effect of the surfactant concentration on the extraction efficiency, droplets generated using different concentrations of surfactant, ranging from 0.005 to 1%, are tested. The results indicate that when the surfactant

concentration is below 0.02%, droplet coalescence occurs due to the unstable water-oil interface; when the surfactant concentration is above 0.2%, the droplets remain separated from the PEG-rich solution after complete oil evaporation (Fig. 3c, d). Thus, the surfactant concentration should be kept at appropriate ranges to stabilize the interface and release the core droplets. Using 0.05% surfactant as a demonstration, the core droplets can be efficiently extracted within 40 s. Moreover, with this evaporation-driven extraction, the inner core droplets are free from external disturbance and can maintain their uniform shapes and sizes (coefficient of variation of approximately 2%).

Table 3 The core-droplet diameter and generation frequency at different polymer concentrations in the active generation mode

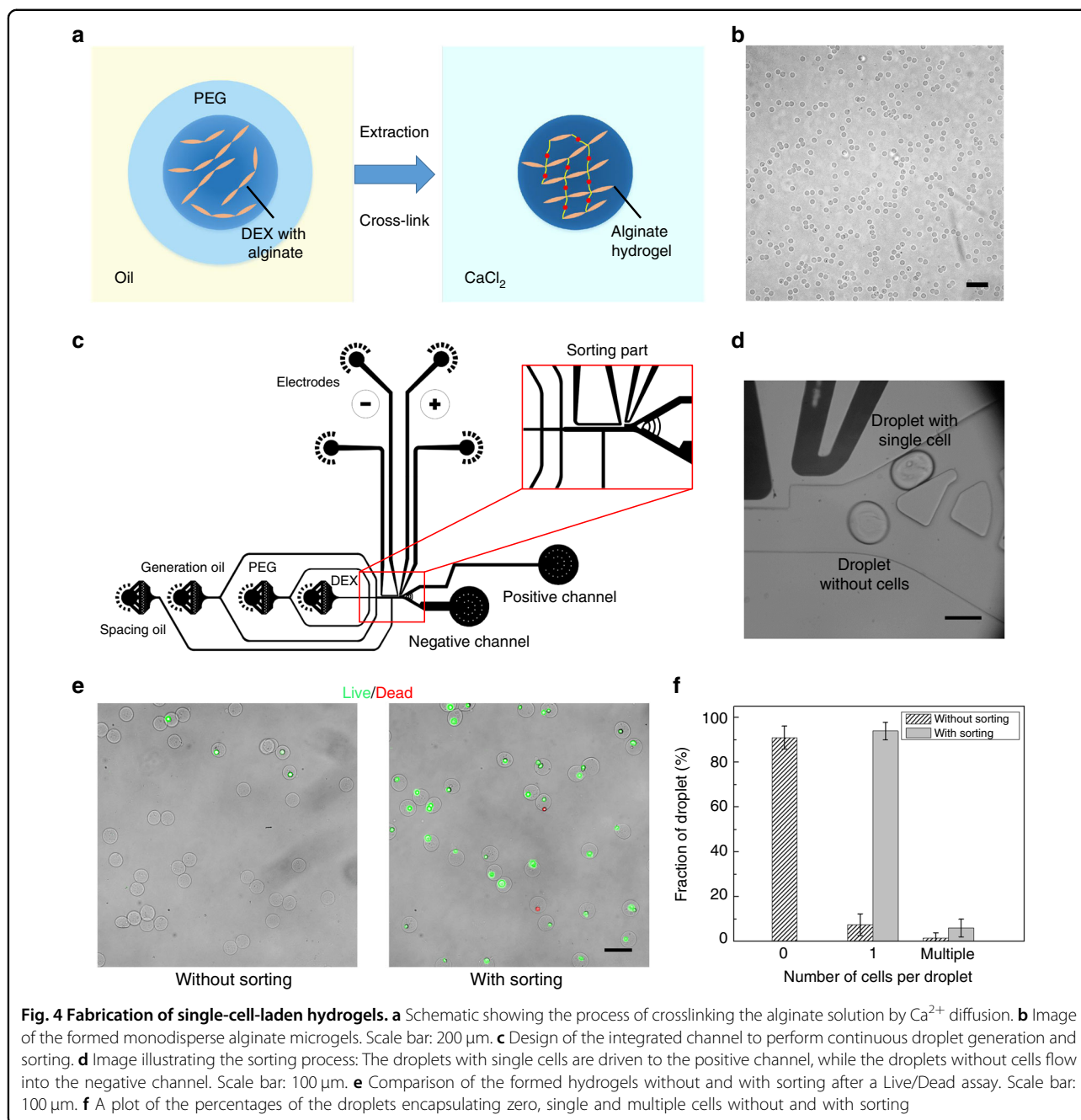
DEX-rich	M _w 8000 (PEG-rich)						
	10%		15%		20%		
	Core size (μm)	Frequency (Hz)	Core size (μm)	Frequency (Hz)	Core size (μm)	Frequency (Hz)	
M _w 10,000	10%	52.2 ± 0.8	747.0 ± 30.1	54.6 ± 0.5	641.8 ± 23.0	56.0 ± 0.7	595.4 ± 16.5
	15%	54.4 ± 0.5	650.2 ± 23.0	56.2 ± 0.8	595.4 ± 16.5	58.6 ± 0.5	538.0 ± 16.4
	20%	57.2 ± 0.8	575.2 ± 17.5	59.2 ± 0.4	520.8 ± 11.6	60.6 ± 0.5	480.8 ± 10.7



Single-cell-laden microgel sorting

Droplet-based hydrogel microspheres, which can provide both mechanical stability and cell-binding properties, are promising scaffolds for 3D cell culture and single-cell analysis^{27,28}. However, the conventional fabrication method

based on a water-oil system requires strong mechanical and chemical treatment to extract the formed hydrogels from organic solvents, possibly resulting in loss of cell viability²⁹. In comparison, the demonstrated ATPS droplet facilitates biocompatible microgel fabrication in an all-aqueous



environment. We achieve this aim by incorporating alginate, a biocompatible polymer that can be physically crosslinked with divalent ions³⁰, into the DEX-rich phase. Through collecting the double emulsions into a calcium chloride (CaCl_2) solution bath, the released core droplets can be rapidly crosslinked to form spherical and uniform-sized hydrogels (Fig. 4a, b).

Moreover, the transient use of the oil phase enables inclusion of a droplet sorting step after double-emulsion generation and before extraction of the core droplets to produce single-cell-laden hydrogels, which is difficult to

achieve in other ATPS droplet generation approaches³¹. We demonstrate this process in an integrated channel composed of both generation and sorting parts (Fig. 4c). Here, a spacing oil flow is introduced to further gap the continuously generated droplets for accurate sorting, and the two branch channels are designed with precise differences in hydraulic resistances. As a result, the droplets are guided into the lower channel when no electric field is applied and are driven into the upper channel when an electric field is applied (Fig. 4d). Through setting the flow rates of the core, shell, generation and spacing oil phases

at 200, 600, 3000 and 3000 $\mu\text{L}/\text{h}$, respectively, high-throughput sorting can be achieved at frequencies above 300 Hz. To demonstrate the sorting-based fabrication of single-cell-laden microgels, the average cell number in each droplet is tuned to 0.1 so that only approximately 10% of the generated droplets contain single cells following the Poisson distribution. With a sorting step to remove the negative droplets, the single-cell encapsulation ratio increases to over 90%, thus allowing a high-throughput analysis of the encapsulated single cells (Fig. 4e, f). Moreover, to verify the biocompatibility of this technique, a live/dead assay is performed on the encapsulated cells and shows high viability, with over 95% of the cells remaining alive. This result suggests that the encapsulated cells can be further cultured for tissue development and engineering applications.

Discussion

The core concept of this technique is to first use oil as a continuous phase to rapidly generate W-W-O double-emulsion drops and then remove the oil to release the inner cores for water-in-water droplet formation. With the use of oil as a continuous phase, sorting can be further incorporated after the formation of double-emulsion drops and before the extraction of core droplets to select the candidates of interest.

In double-emulsion generation, the low interfacial tension that is frequently encountered for water-in-water droplets can be overcome by introducing an oil phase, thus achieving high levels of throughput and monodispersity in both passive and active methods. Through adjusting the flow rates, the morphology of the double-emulsion drops formed can be precisely controlled, and the generation frequency can be as high as ~ 2.4 kHz, which is 20 times higher than that of existing methods. Moreover, the fabricated double-emulsion drops can be used to form ATPS microcapsules by adding hydrogel components into the shell phase, which may serve as biocompatible carriers in drug delivery and food processing assays³².

The approach of active double-emulsion formation through sequential droplet injection is efficient for performing controlled reactions within the inner droplets, which is not limited to the demonstrated sample mixing and can be extended to other functional operations. For instance, through the incorporation of different individual cells by sequential injections, cell-to-cell communications and interactions at the single-cell level can be studied within biocompatible compartments. Moreover, if we further increase the gap between each injector or perform sequential injections in separate devices, the core droplet can be stabilized before subsequent injection, thus forming double emulsions with multiple separate cores. This type of structure is potentially applied in fabricating cell-like

biomimetic architectures, such as protocells, where the core droplets can function as independent artificial organelles.

To gently break the double emulsions without damaging the inner cores, an oil evaporation-based method is introduced, enabling fabrication of monodisperse ATPS droplets with spherical shapes. The obtained all-aqueous microspheres can serve as biocompatible templates to perform various assays, as demonstrated in the microgel particle fabrication and DNA partitioning studies. Moreover, the employed core-release method is useful for recovering single-emulsion drops, which can be functionalized to extract the encapsulated single cells from water-in-oil droplets⁴.

When combined with accurate droplet sorting, the demonstrated production of single-cell-laden hydrogels promises further high-throughput analysis of the encapsulated single cells, such as detecting their immune responses to study the distribution of antibiotic resistance and monitoring their differentiation to probe the heterogeneity among populations. Moreover, noninvasive operations guarantee high cell viability, enabling further culture to develop microgels into functional building blocks for bottom-up tissue engineering³³.

Despite the high efficiency of this method in generating and sorting ATPS droplets, there is still room to further exploit its potential. For instance, the finally formed droplets are still in a single-emulsion format, which restricts their use in applications that require controlled sample encapsulation and release³⁴. Thus, further development should focus on the fabrication of more functional aqueous multiple-emulsion drops, which may be achieved by the introduction of additional immiscible aqueous flows for compartmentation.

In summary, the introduction of a transient oil medium enables high-throughput generation and sorting of water-in-water droplets, which can be used as templates to encapsulate single cells in hydrogel microspheres. The simplicity, high throughput and capacity to be integrated into more sophisticated microfluidic processes inspire new ways to use these droplets in various material synthesis and biological analyses.

Materials and methods

ATPS droplet generation

To prepare ATPS solutions, PEG (M_w 8000, Sigma-Aldrich, USA) and DEX (M_w 10,000, Sigma-Aldrich, USA) polymers were dissolved in deionized water at weight ratios from 10 to 20%. After centrifugation at 8000 rpm for 1 h, the solutions were left standing overnight to achieve complete separation. Then, the equilibrated PEG-rich and DEX-rich solutions were collected separately, and the polyelectrolytes, PSS and PAH (Sigma-Aldrich, USA), were dissolved into the two phases at

concentrations of 2 mg/mL. For further fluorescent labeling in the sequential injection studies, fluorescein isothiocyanate-dextran (M_w 10,000, Sigma-Aldrich, USA) was dissolved into the DEX-rich phase at a weight ratio of 0.5%. A fluorinated oil (HFE7500, 3M, USA) was used as the continuous phase for droplet generation, and the weight ratios of a fluorosurfactant (008, RAN Biotechnologies, USA) were varied from 0.005 to 1%. To form alginate hydrogels, an alginic acid sodium salt from brown algae (low viscosity, Sigma-Aldrich, USA) was dissolved into the DEX-rich phase at a weight ratio of 1%, and a 1% weight ratio of CaCl_2 solution (Aladdin, CN) was used to extract the core droplets.

Device fabrication

The microfluidic devices were fabricated using a typical soft lithography replica molding technique³⁵. First, a channel mold was fabricated on a silicon wafer (N100, University, USA) with SU-8 photoresist (2025, Micro-Chem, USA) using maskless lithography (SF-100 Xcel, Intelligent Micro Patterning, LLC, USA). Then, the PDMS prepolymer base (Sylgard 184, Dow Corning, USA) was crosslinked with the curing agent at a weight ratio of 10:1. After sufficient mixing by a conditioning mixer (AR-100, THINKY, JP), the mixture was poured onto a channel mold and cured at 65 °C for 4 h. Subsequently, the PDMS channel was peeled off from the mold. Finally, after inlet and outlet punching, the PDMS channel was bonded to a glass substrate (ISOLAB, DE) through oxygen plasma treatment (PDC-002, Harrick, USA) and heated at 90 °C for 2 h. The height, width and length of the generation channel were designed to be 65, 120 and 2000 μm , respectively, and the whole channel was treated with a hydrophobic agent (Aquapel, PPG, USA) to guarantee stable droplet generation. To fabricate the electrodes required in active generation and sorting, empty channels were fabricated in the desired shape of the electrodes. Then, a low-melting-point metal wire (52225, Indium Incorporation, USA) was inserted into the electrode channel from one end at 95 °C, and negative pressure was applied to the other end to fill the whole channel with liquid metal. After further cooling the device to solidify the metal, metallic electrodes could be formed according to the desired shape.

Cell assay

An esophageal cancer cell line (KYSE-150) was used as the target encapsulant to test the sorting efficiency. For fluorescence labeling, the cells were transduced with lentiviral particles encoding green fluorescent protein (GFP). The coding sequence was cloned into a pLVX-puro backbone (Clontech, USA) following an EF-2 alpha promoter³⁶. The cells were maintained in Roswell Park Memorial Institute (RPMI) 1640 Medium (Life Technologies, USA), 100 U/mL penicillin and 100 $\mu\text{g}/\text{mL}$ streptomycin (Gibco,

USA) in a humidified atmosphere at 37 °C with 5% CO_2 . After trypsin treatment, the cells were transferred into the prepared DEX-alginate solution at a concentration of $3.05 \times 10^6/\text{mL}$. The cell viability after encapsulation and sorting was tested using a Live/Dead reagent (calcein AM/ethidium homodimer-1, Sigma-Aldrich, USA).

Droplet sorting

A typical fluorescence-activated droplet sorting (FADS) system was used to sort the double-emulsion drops with single cells^{37,38}. A diode-pumped solid-state (DPSS) laser source (20 mW, CNI, CN), with a wavelength of 488 nm, was used to excite the fluorescence signal. Guided by a dichroic mirror (Semrock, USA), the laser beam was reflected into a plan fluorite objective (Olympus, JP) and focused into the microfluidic channel. Then, the excited fluorescence signal propagated backward and was separated into two beams through a beam splitter (Thorlabs, USA), with 90% of the light received by a photomultiplier tube (PMT, Hamamatsu, JP) for fluorescence detection and the remaining 10% used for high-speed imaging (Phantom V9.1, Vision Research, USA). Subsequently, the triggered signal was processed by a custom LabVIEW program (PCI-e 7842R, National Instruments, USA), responding with output signals applied to the electrodes after amplification by a high-voltage amplifier (5/80, Trek, USA).

Acknowledgements

This work was supported by the General Research Fund (Nos. 17307919, 17329516, 17304017, 17305518, and 17306315) and the Research Impact Fund (No. R7072-18) from the Research Grants Council of Hong Kong, Excellent Young Scientists Fund (Hong Kong and Macau) (21922816) from the National Natural Science Foundation of China (NSFC) as well as the Seed Fund for Basic Research (Nos. 201811149241, 201711159249, and 201611159205), the Seed Fund for Translational and Applied Research (No. 201711160016) and Platform Technology Funding from the University of Hong Kong. We thank Prof. Maria Li Lung from HKU's Department of Clinical Oncology for providing the KYSE-150 cell samples, Ph.D. candidate Yage Zhang for the assistance in cell culture, and Dr. Youchuang Chao for the discussion of ATPS solution preparation.

Author contributions

L.N. and H.C.S. conceived the project, and Y.C. prepared the ATPS and cell samples. S.Y. designed and fabricated the devices. L.N. performed the experiments, and Y.C. analyzed the results. L.N. and H.C.S. wrote the manuscript.

Conflict of interest

The authors declare that they have no conflict of interest.

Supplementary information accompanies this paper at <https://doi.org/10.1038/s41378-020-0180-0>.

Received: 25 January 2020 Revised: 17 April 2020 Accepted: 6 May 2020
Published online: 07 September 2020

References

1. Shang, L., Cheng, Y. & Zhao, Y. Emerging droplet microfluidics. *Chem. Rev.* **117**, 7964–8040 (2017).
2. Yu, Y. et al. Microfluidic lithography of bioinspired helical micromotors. *Angewandte Chemie* **129**, 12295–12299 (2017).

3. Yu, Y., Guo, J., Sun, L., Zhang, X. & Zhao, Y. Microfluidic generation of micro-springs with ionic liquid encapsulation for flexible electronics. *Research* **2019**, 6906275 (2019).
4. Nan, L., Lai, M. Y. A., Tang, M. Y. H., Chan, Y. K., Poon, L. L. M. & Shum, H. C. On-demand droplet collection for capturing single cells. *Small* **16**, 1902889 (2020).
5. Fidalgo, L. M. et al. From microdroplets to microfluidics: selective emulsion separation in microfluidic devices. *Angewandte Chemie* **120**, 2072–2075 (2008).
6. Song, Y. et al. Fabrication of fibrillosomes from droplets stabilized by protein nanofibrils at all-aqueous interfaces. *Nat. Commun.* **7**, 12934 (2016).
7. Chan, Y. K., Yan, W. H., Hung, L. T., Chao, Y., Wu, J. & Shum, H. C. All-Aqueous Thin-Film-Flow-Induced Cell-Based Monolayers. *ACS Appl. Mat. Interfaces* **11**, 22869–22877 (2019).
8. Chao, Y. & Shum, H. C. Emerging aqueous two-phase systems: from fundamentals of interfaces to biomedical applications. *Chem. Soc. Rev.* **49**, 114–142 (2020).
9. Frampton, J. P., White, J. B., Abraham, A. T. & Takayama, S. Cell co-culture patterning using aqueous two-phase systems. *J. Visual. Exp.* **73**, e50304 (2013).
10. Song, Y. et al. Budding-like division of all-aqueous emulsion droplets modulated by networks of protein nanofibrils. *Nat. Commun.* **9**, 2110 (2018).
11. Dewey, D. C., Strulson, C. A., Cacace, D. N., Bevilacqua, P. C. & Keating, C. D. Bioreactor droplets from liposome-stabilized all-aqueous emulsions. *Nat. Commun.* **5**, 4670 (2014).
12. Chao, Y., Mak, S. Y., Rahman, S., Zhu, S. & Shum, H. C. Generation of high-order all-aqueous emulsion drops by osmosis-driven phase separation. *Small* **14**, 1802107 (2018).
13. Moon, B.-U., Abbasi, N., Jones, S. G., Hwang, D. K. & Tsai, S. S. Water-in-water droplets by passive microfluidic flow focusing. *Anal. Chem.* **88**, 3982–3989 (2016).
14. Hardt, S. & Hahn, T. Microfluidics with aqueous two-phase systems. *Lab Chip* **12**, 434–442 (2012).
15. Ma, Q. et al. Partitioning-dependent conversion of polyelectrolyte assemblies in an aqueous two-phase system. *Soft Matter* **14**, 1552–1558 (2018).
16. Mak, S. Y., Chao, Y., Rahman, S. & Shum, H. C. Droplet formation by rupture of vibration-induced interfacial fingers. *Langmuir* **34**, 926–932 (2017).
17. Zhou, C. et al. Microfluidic generation of aqueous two-phase-system (ATPS) droplets by oil-droplet choppers. *Lab Chip* **17**, 3310–3317 (2017).
18. Caen, O. et al. High-throughput multiplexed fluorescence-activated droplet sorting. *Microsyst. Nanoeng.* **4**, 33 (2018).
19. Yuan, H. et al. Pico-injection-enabled multitarget loop-mediated isothermal amplification for detection of foodborne pathogens. *Anal. Chem.* **90**, 13173–13177 (2018).
20. Moon, B.-U., Jones, S. G., Hwang, D. K. & Tsai, S. S. Microfluidic generation of aqueous two-phase system (ATPS) droplets by controlled pulsating inlet pressures. *Lab Chip* **15**, 2437–2444 (2015).
21. Liu, H. T. et al. A microfluidic strategy for controllable generation of water-in-water droplets as biocompatible microcarriers. *Small* **14**, 1801095 (2018).
22. Mazutis, L. et al. Single-cell analysis and sorting using droplet-based microfluidics. *Nat. Protoc.* **8**, 870–891 (2013).
23. Wang, H. et al. One-step generation of core-shell gelatin methacrylate (GelMA) microgels using a droplet microfluidic system. *Adv. Mater. Technol.* **4**, 1800632 (2019).
24. Abate, A. & Weitz, D. High-order multiple emulsions formed in poly (dimethylsiloxane) microfluidics. *Small* **5**, 2030–2032 (2009).
25. Abate, A. R., Hung, T., Mary, P., Agresti, J. J. & Weitz, D. A. High-throughput injection with microfluidics using picoinjectors. *Proc. Natl Acad. Sci. USA* **107**, 19163–19166 (2010).
26. Rotem, A. et al. Single-cell ChIP-seq reveals cell subpopulations defined by chromatin state. *Nat. Biotechnol.* **33**, 1165 (2015).
27. Mao, A. S. et al. Deterministic encapsulation of single cells in thin tunable microgels for niche modelling and therapeutic delivery. *Nat. Mater.* **16**, 236 (2017).
28. Nan, L., Yang, Z., Lyu, H., Lau, K. Y. Y. & Shum, H. C. A microfluidic system for one-chip harvesting of single-cell-laden hydrogels in culture medium. *Adv. Biosyst.* **3**, 1900076 (2019).
29. Martinez, C. J. et al. A microfluidic approach to encapsulate living cells in uniform alginate hydrogel microparticles. *Macromol. Biosci.* **12**, 946–951 (2012).
30. Lee, K. Y. & Mooney, D. J. Hydrogels for tissue engineering. *Chem. Rev.* **101**, 1869–1880 (2001).
31. Ziemecka, I. et al. Monodisperse hydrogel microspheres by forced droplet formation in aqueous two-phase systems. *Lab Chip* **11**, 620–624 (2011).
32. Shum, H. C., Kim, J.-W. & Weitz, D. A. Microfluidic fabrication of monodisperse biocompatible and biodegradable polymersomes with controlled permeability. *J. Am. Chem. Soc.* **130**, 9543–9549 (2008).
33. Khademhosseini, A. & Langer, R. A decade of progress in tissue engineering. *Nat. Protoc.* **11**, 1775 (2016).
34. Datta, S. S. et al. 25th anniversary article: double emulsion templated solid microcapsules: mechanics and controlled release. *Adv. Mater.* **26**, 2205–2218 (2014).
35. Qin, D., Xia, Y. & Whitesides, G. M. Soft lithography for micro-and nanoscale patterning. *Nat. Protoc.* **5**, 491 (2010).
36. Yu, V. Z. et al. Nuclear localization of DNAJB6 is associated with survival of patients with esophageal cancer and reduces AKT signaling and proliferation of cancer cells. *Gastroenterology* **149**, 1825–1836.e1825 (2015).
37. Baret, J.-C. et al. Fluorescence-activated droplet sorting (FADS): efficient microfluidic cell sorting based on enzymatic activity. *Lab Chip* **9**, 1850–1858 (2009).
38. Tang, M. Y. & Shum, H. C. One-step immunoassay of C-reactive protein using droplet microfluidics. *Lab Chip* **16**, 4359–4365 (2016).